ICSV14
Cairns • Australia
9-12 July, 2007

14th International Congress on Sound & Vibration

MODELLING OF FLOATING-SLAB TRACKS WITH DISCONTINUOUS SLABS IN UNDERGROUND RAILWAY TUNNELS

Mohammed Hussein[1] and Hugh Hunt[2]

[1]School of Civil Engineering, University of Nottingham
Coates Building, University Park, Nottingham, NG7 2RD, UK
[2]Engineering Department, University of Cambridge
Trumpington Street, Cambridge, CB2 1PZ, UK
Email address: mohammed.hussein@nottingham.ac.uk

Abstract

Floating-slab tracks are known as effective means for isolating vibration from underground railway tunnels. Slabs are supported on tunnels via rubber bearings or steel springs. The slab can be continuous or discontinuous. Continuous slab is cast in-situ and discontinuous slab is constructed in discrete pre-cast sections. A track with discontinuous slab exhibits more resonances due to constructive interference of waves that reflect at both ends of the slab.
This paper presents a new method for modelling floating-slab tracks with discontinuous slabs in underground railway tunnels. The track is subjected to a harmonic moving load. The model consists of two sub-models. The first is an infinite track with periodic double-beam unit formulated as a periodic infinite structure. The second is modelled with a new version of the Pipe-in-Pipe (PiP) model that accounts for a tunnel wall embedded in a half-space. The two sub-models are coupled by writing the force transmitted from the track to the tunnel as a continuous function using Fourier series representation and satisfying the displacement compatibility.
The displacements at the free surface are calculated for a track with discontinuous slab and compared with those of a track with continuous slab. The results confirm that the far-field vibration can significantly be increased due to resonance frequencies of slab for tracks with discontinuous slabs.

1. INTRODUCTION

Vibration from underground railways can be reduced by using floating-slab tracks. The track is isolated from the track bed via rubber bearings or steel springs. The slab can be cast in-situ leading to a track with a continuous slab. It may also be constructed in discrete pre-cast sections leading to a track with a discontinuous slab. The latter track has more resonances than the former due to constructive interference of bending waves which reflects at free ends of slab.
Floating-slab tracks with discontinuous slabs on rigid foundations are modelled by Hussein

and Hunt [1,2]. These models are useful in understanding the dynamic effect of slab discontinuity on vibration induced at the track bed. However, a comprehensive model of the tunnel and the soil is important to account for the track-tunnel interaction and to provide the necessary transfer functions for the calculations of the far-field response due to a load applied on the track.

In this paper, a model of a floating-slab track with discontinuous slab resting on a tunnel embedded in a half-space is presented. The Euler-Bernoulli beam theory is used to account for the flexural behaviour of the track. The periodic-infinite structure theory is employed to account for periodicity of the model. The tunnel and the ground is modelled using the new version of the Pipe-in-Pipe (PiP) model [3,4] which accounts accurately for a circular tunnel embedded in a half-space.

This paper is organised in the following sections. Section 2 presents the model formulation. Section 3 presents results of the model where the response in the free-surface due to a harmonic load moving on the track with a constant velocity is shown and compared to those resulting from a track with a continuous slab.

2. FORMULATION OF THE MODEL

The model used in this paper is shown in Figure 1. The two rails of the track are modelled as a single Euler-Bernoulli beam which is supported on a slab via continuous layer of springs to account for railpads. The slab is modelled as Euler-Bernoulli beam supported on the tunnel invert via another layer of springs to account for slab bearings. The tunnel and soil are formulated using the PiP model [3-6]. The PiP model accounts for a tunnel embedded in a half-space by using the elastic continuum theory for a tunnel in a full-space along with Green's functions for an elastic half-space.

For the model shown in Figure 1, the governing equations of the unit of the track in the range ($0 \le x \le L$), in the frequency domain, can be written in the form [1]

$$EI_1 \frac{\partial^4 \tilde{y}_1}{\partial x^4} - m_1 \omega^2 \tilde{y}_1 + k_1(\tilde{y}_1 - \tilde{y}_2) = \frac{1}{v} e^{i\frac{(\varpi-\omega)}{v}x}, \tag{1}$$

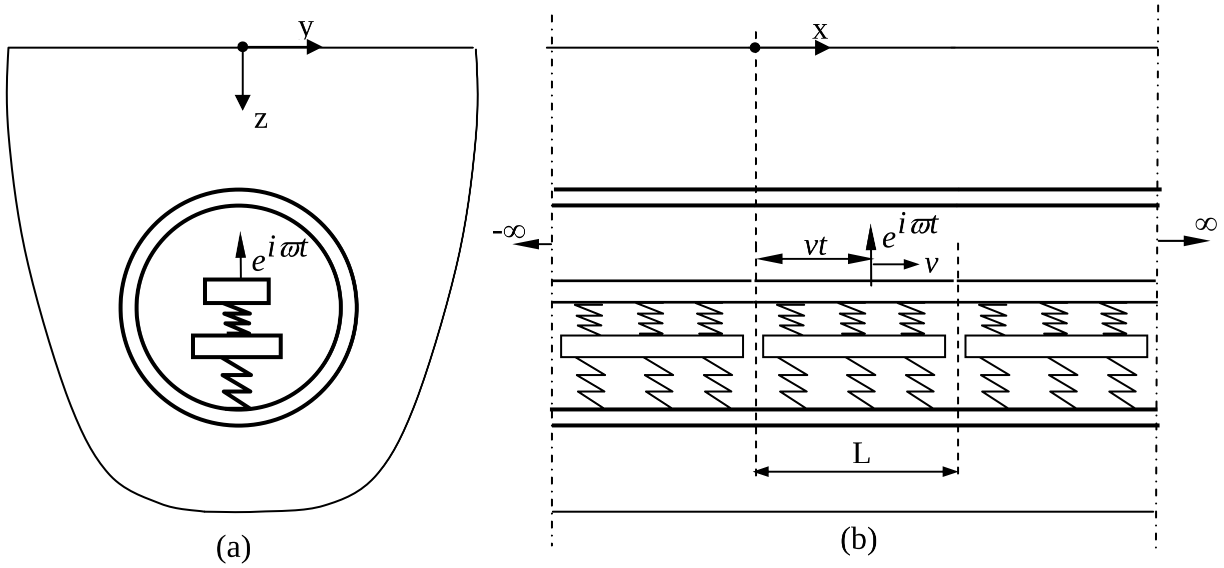

Figure 1: A model of a floating-slab track with discontinuous slab subjected to a harmonic load moving with a constant velocity along the track. (a) End view. (b) Side view.

$$EI_2 \frac{\partial^4 \tilde{y}_2}{\partial x^4} - m_2 \omega^2 \tilde{y}_2 - k_1(\tilde{y}_1 - \tilde{y}_2) = -\tilde{R}\,, \tag{2}$$

$$\tilde{R} = k_2(\tilde{y}_2 - \tilde{y}_3)\,, \tag{3}$$

with boundary conditions

$$\frac{\partial^k \tilde{y}_1(L,\omega)}{\partial x^k} = e^{i(\frac{\varpi-\omega}{v})L} \frac{\partial^k \tilde{y}_1(0,\omega)}{\partial x^k}\,, \text{ for } k = 0,1,2,3 \tag{4}$$

$$\frac{\partial^k \tilde{y}_2(L,\omega)}{\partial x^k} = \frac{\partial^k \tilde{y}_2(0,\omega)}{\partial x^k} = 0\,, \text{ for } k = 2,3 \tag{5}$$

where $\tilde{y}_1$, $\tilde{y}_2$ and $\tilde{y}_3$ are the displacement of the rails, the slab, the track bed, i.e. the tunnel respectively. $\tilde{R}$ is the induced force between the track and the tunnel. All the previous quantities are functions of space x and frequency ω. EI_1 and EI_2 are the bending stiffness of the rails (for two rails) and the slab respectively. m_1 and m_2 are the mass per unit length of the rails (for two rails) and the slab respectively. k_1 and k_2 are the stiffness per unit length of the railpads (for two rails) and the slab bearings respectively. ϖ and v are the excitation frequency and the velocity of the moving load.

According to the periodic-structure theory, the force on the tunnel invert satisfies the following relationship

$$\tilde{R}(x+L,\omega) = e^{i(\frac{\varpi-\omega}{v})L} \tilde{R}(x,\omega)\,. \tag{6}$$

Equation 6 shows that $\tilde{R}$ is a periodic function of the second kind which can be transformed into an equation with periodicity of the first kind using the following substitution

$$\tilde{Q}(x,\omega) = e^{-i(\frac{\varpi-\omega}{v})x} \tilde{R}(x,\omega)\,. \tag{7}$$

From equations 6 and 7, one can write

$$\tilde{Q}(x+L,\omega) = \tilde{Q}(x,\omega)\,. \tag{8}$$

Equation 8 shows that $\tilde{Q}$ is a periodic function of the first kind. This equation can be written as a summation of Fourier series, see [7] for example. The resulting expression can be substituted in equation 7 to get

$$\tilde{R}(x,\omega) = \sum_{n=-\infty}^{n=\infty} b_n(\omega) \cdot e^{i(\xi_n + \frac{\varpi}{v} - \frac{\omega}{v})x} \text{ with } \xi_n = \frac{2\pi n}{L}\,. \tag{9}$$

Equation 9 can be used to write the displacement of the track bed as

$$\tilde{y}_3(x,\omega)=\sum_{n=-\infty}^{n=\infty} b_n(\omega)\cdot \tilde{H}_t(\xi_n+\frac{\varpi}{v}-\frac{\omega}{v},\omega)\, e^{i(\xi_n+\frac{\varpi}{v}-\frac{\omega}{v})x} \tag{10}$$

where $\tilde{H}_t(\xi,\omega)$ is the Frequency Response Function (FRF) of the tunnel, i.e. the displacement of the tunnel due to a unit excitation on the tunnel in the wavenumber-frequency domain. To calculate the displacement at any point in the soil, the FRF on the right hand side of equation 10 is replaced by the transfer function between that point and the tunnel.

The purpose of the rest of analysis is to determine the coefficients $b_n(\omega)$ for given parameters of the track and for a prescribed ϖ and v. Equations 1 and 2 can be written in the following form (using equation 9 to substitute for $\tilde{R}$)

$$\begin{bmatrix} EI_1 & 0 \\ 0 & EI_2 \end{bmatrix}\frac{\partial^4 \tilde{y}}{\partial x^4}+\begin{bmatrix} k_1-m_1\omega^2 & -k_1 \\ -k_1 & k_1-m_2\omega^2 \end{bmatrix}\tilde{y}=\begin{bmatrix} 0 \\ 0 \end{bmatrix}+\begin{bmatrix} 1 \\ 0 \end{bmatrix}(1/v)e^{i\frac{(\varpi-\omega)}{v}x}-\sum_{n=-\infty}^{n=\infty}\begin{bmatrix} 0 \\ 1 \end{bmatrix} b_n(\omega)e^{i(\xi_n+\frac{\varpi}{v}-\frac{\omega}{v})x} \tag{11}$$

where $\tilde{y}(x,\omega)=[\tilde{y}_1(x,\omega),\tilde{y}_2(x,\omega)]^T$. The solution of equation 11 is written as a superposition of solutions resulting from each term of the right hand side expression. Note that the solution due to the first term in the right hand side expression of equation 11 is the homogeneous solution of the differential equations. The complete solution reads

$$\tilde{y}(x,\omega)=\sum_{j=1}^{j=8} a_j \tilde{Y}_j e^{i\phi_j x}+\tilde{U}\cdot e^{i(\frac{\varpi}{v}-\frac{\omega}{v})x}+\sum_{n=-\infty}^{n=\infty} V_n b_n e^{i(\xi_n+\frac{\varpi}{v}-\frac{\omega}{v})x} \tag{12}$$

where a_j and $\tilde{Y}_j$ are the coefficients and the eigenvectors of the homogeneous solution. $\tilde{U}$ and V_n are the vectors of coefficients of the particular solutions. Equation 12 is defined in the range ($0\le x\le L$). However $\tilde{y}(x,\omega)$ satisfies the following relationship

$$\tilde{y}(x+L,\omega)=e^{i(\frac{\varpi-\omega}{v})x}\tilde{y}(x,\omega) \tag{13}$$

Due to the periodicity of the second kind in equation 13, equation 12 can be written for all values of x, even outside the range ($0\le x\le L$), using Fourier series representation as

$$\tilde{y}(x,\omega)=\sum_{n=-\infty}^{n=\infty}\sum_{j=1}^{j=8} ia_j\tilde{Y}_j[\frac{e^{-i(\xi_n-\phi_j+\varpi/v-\omega/v)L}-1}{(\xi_n-\phi_j+\varpi/v-\omega/v)L}]e^{i(\xi_n-\phi_j+\varpi/v-\omega/v)x}+\tilde{U}e^{i(\frac{\varpi}{v}-\frac{\omega}{v})x}+\sum_{n=-\infty}^{n=\infty} V_n b_n e^{i(\xi_n+\frac{\varpi}{v}-\frac{\omega}{v})x} \tag{14}$$

Considering only a limited number of terms ($-n_{\max}\le n\le n_{\max}$), the previous equation has $2n_{\max}+9$ unknown; $(b_{-n_{\max}}, b_{-n_{\max}+1},..., b_0,..., b_{n_{\max}-1}, b_{n_{\max}})$ and $(a_1,a_2,...,a_8)$.

Substituting $\tilde{y}_2$ and $\tilde{y}_3$ from equations 14 and 10 respectively into equation 3 and equating the resulting expression of $\tilde{R}$ to the one in equation 9 gives

$$\sum_{j=1}^{j=8} ia_j \tilde{Y}_j(2,1)[\frac{e^{-i(\xi_n-\phi_j+\varpi/v-\omega/v)L}-1}{(\xi_n-\phi_j+\varpi/v-\omega/v)L}]+\tilde{U}(2,1)+b_n[V_n(2,1)-\tilde{H}_t(\xi_n+\frac{\varpi}{v}-\frac{\omega}{v},\omega)-1/k_2]=0 \quad \text{for any n} \quad (15)$$

The last equation along with the eight boundary conditions represent the necessary $2n_{\max}+9$ equations to calculate all the unknowns b_n and a_j. Using these values, equation 10 is employed to calculate the response at any position in the soil by using the suitable FRF from the PiP model as discussed before. The displacements in the space-frequency domain are transformed to the space-time domain using the Discrete Fourier transform.

4. SAMPLE RESULTS

In this section the displacement results at the free-surface due to a harmonic force moving on the track with a constant velocity v = 40 km/hr are presented. The following parameters are used for the analysis. For the track, EI_1=10 MPa.m^4, m_1= 100 kg/m, EI_2=1430 MPa.m^4, m_2=3500 kg/m, k_1=20 MN/m/m (with hysteretic loss factor of η_{k1}=0.3), k_2=5 MN/m/m (with hysteretic loss factor of η_{k2}=0.5). The track has a discontinuous slab of length L=6m. For the tunnel, external radius r_2= 3.0 m, internal radius r_1= 2.75 m, compression wave velocity c_1= 5189 m/s, shear wave velocity c_2= 2774 m/s, density ρ= 2500 kg/m^3 (with hysteretic loss factor of η=0.015 associated with both pressure and shear wave velocities). The distance between the tunnel centre and the free surface is 20m. For the soil, compression wave velocity c_1= 944 m/s, shear wave velocity c_2= 309 m/s, density ρ= 2000 kg/m^3 (with hysteretic loss factor of η=0.03 associated with both pressure and shear wave velocities).

The displacements of the track with discontinuous slab are compared with those of a track with a continuous slab. The latter results are calculated using a continuous model of a track-tunnel-soil formulated in the wavenumber-frequency domain and results are then transformed to the space-time domain.

Figure 2 shows the displacements in the free-surface at (x=0, y=0, z=0) in the frequency domain due to a harmonic load with excitation frequency 10Hz and moving on a floating slab track with continuous and discontinuous slabs (see Figure 1 for information about the coordinate systems). It can be seen that the displacements are large at frequencies close to the excitation frequency, i.e. 10 Hz. Around this frequency, both tracks give the same displacements and the difference between the two curves becomes large at frequencies away from the excitation frequency.

It can also be observed that the displacements for a track with a continuous slab decay more quickly away from the excitation frequency compared with those for a track with a discontinuous slab. Figure 3 shows the displacements in the free-surface at the same point (x=0, y=0, z=0) in the frequency domain due to a harmonic load with excitation frequency 100Hz and moving on a floating slab track with continuous and discontinuous slabs. The frequency content of the displacements again exhibit large displacements around the excitation frequency and the displacements due to a slab with a continuous slab decays more quickly compared to those for a track with a discontinuous slab.

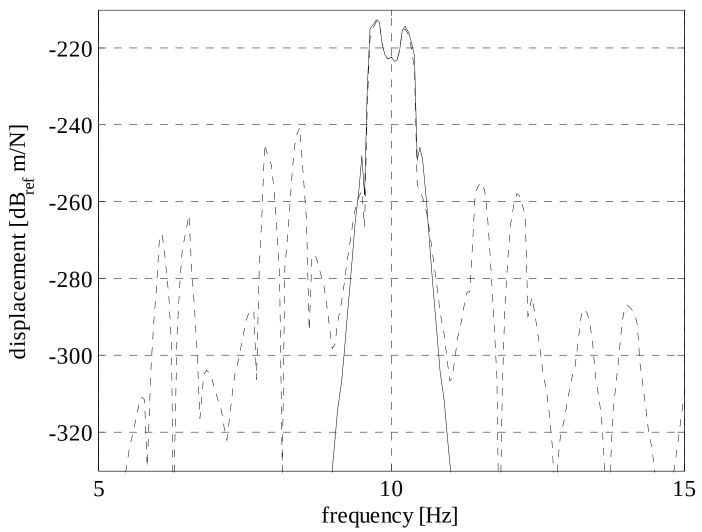

Figure 2: The displacement at x=0, y=0, z=0 due to a harmonic load with frequency 10Hz moving with a constant velocity 40km/hr on (-) a track with continuous slab and (…) a track with a discontinuous slab.

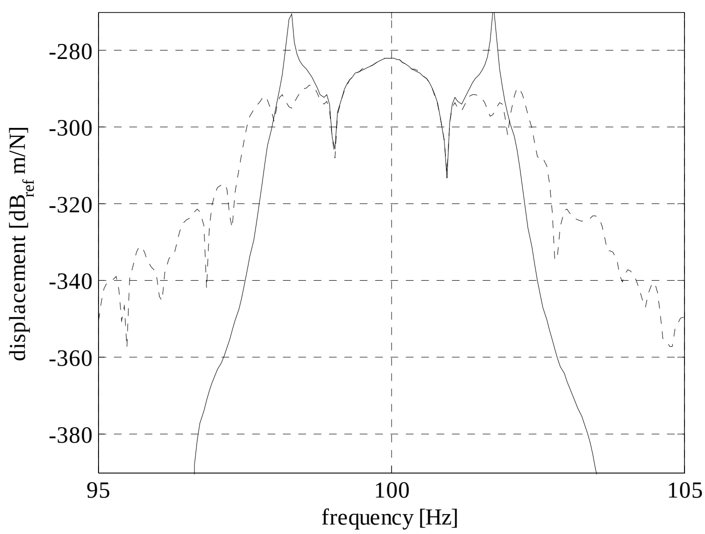

Figure 3: The displacement at x=0, y=0, z=0 due to a harmonic load with frequency 100 Hz moving with a constant velocity 40km/hr on (-) a track with continuous slab and (…) a track with a discontinuous slab.

Figures 4 and 5 show the maximum displacements at two points in the free surface (x=0, y=0, z=0) and (x=0, y=10, z=0) respectively for excitations frequencies in the range 1-200Hz. At each excitation frequency, displacements are calculated in the frequency domain as demonstrated in section 2. Results are then transformed to the time domain and the maximum displacement is recorded. The process is then repeated for all excitations frequencies in the frequency range of interest to produce the results in Figures 4 and 5.

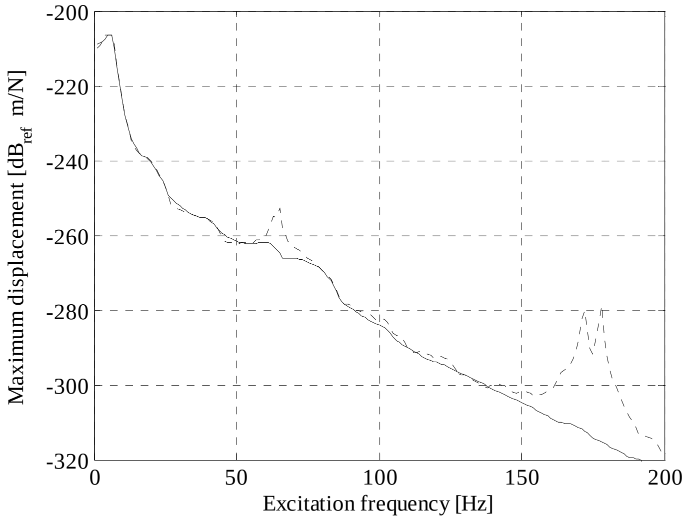

Figure 4: The max. displacement at x=0, y=0, z=0 due to a harmonic load moving with a constant velocity 40km/hr on (-) a track with continuous slab and (…) a track with a discontinuous slab.

It can be seen from Figures 4 and 5 that the displacements for the track with the discontinuous slab have two pronounced peaks at 63 Hz and 174 Hz. At these frequencies, displacements at the free-surface from the track with the discontinuous slab are more than 10 dB larger than those resulting from the track with the continuous slab. The peaks are attributed to standing waves which are built by reflections of propagating waves at free ends of the slab. The frequencies of these peaks can be calculated from the free-free beam natural frequencies, see [8] for example, which reads

$$f_n = \sqrt{\frac{EI_2}{m_2}} \frac{\lambda_n^2}{2\pi L^2} \tag{16}$$

where $\lambda_1 = 4.73$, $\lambda_2 = 7.853$, $\lambda_3 = 10.996$, *etc…*

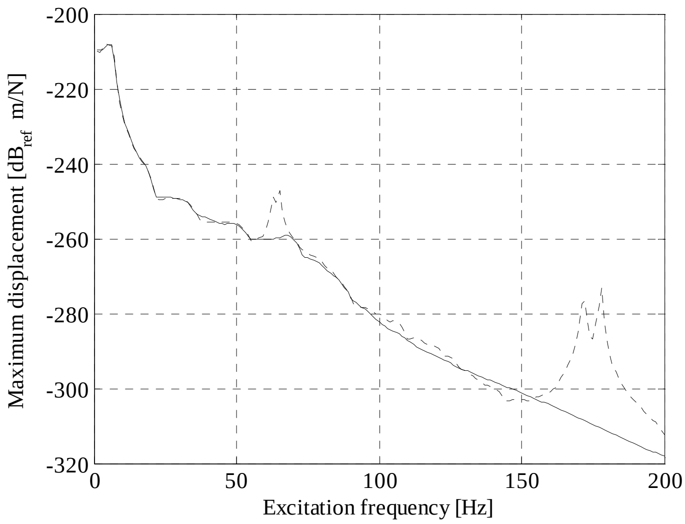

Figure 5: The max. displacement at x=0, y=10, z=0 due to a harmonic load moving with a constant velocity 40km/hr on (-) a track with continuous slab and (…) a track with a discontinuous slab.

For the current parameters of the track, the first two natural frequencies occur at 63.2 and 174.2 Hz, which agree with the results in Figures 4 and 5.

5. CONCLUSIONS

A new model for calculating vibration from floating-slab tracks with discontinuous slabs in underground railway tunnels is presented. The model is based on the periodic-infinite structure theory and Euler-Bernoulli beam theory to account for the track. A tunnel wall embedded in an elastic half-space is modelled using the PiP model. The displacements at the free-surface are calculated and compared with those of tracks with continuous slabs. A floating-slab track with a discontinuous slab results into more vibration at the resonance frequencies of the slab. These frequencies can be calculated using the equation of the natural frequencies of a free-free beam.

REFERENCES

[1] M.F.M. Hussein and H.E.M. Hunt, “Modelling of Floating-Slab track with Discontinuous Slab, Part I: Response to Oscillating Moving Loads”, *Journal of Low Frequency Noise, Vibration and Active Control* **25(1)**, 23-40 (2006).

[2] M.F.M. Hussein and H.E.M. Hunt, “Modelling of Floating-Slab track with Discontinuous Slab, Part 2: response to moving trains”, *Journal of Low Frequency Noise, Vibration and Active Control* **25(2)**, 111-118 (2006).

[3] M.F.M. Hussein, S. Gupta, H.E.M. Hunt, G. Degrande and J.P. Talbot, “An efficient model for calculating vibration from a railway tunnel buried in a half-space”, *Proceeding of the thirteenth International Congress on Sound and Vibration* (ICSV13), 2-6 July 2006, Vienna, Austria.

[4] M.F.M. Hussein, S. Gupta, H.E.M. Hunt, G. Degrande and J.P. Talbot, “A computationally efficient model for calculating vibration from a railway tunnel buried in a half-space”, *International Journal for Numerical Methods in Engineering*, submitted for publication.

[5] J.A. Forrest and H.E.M. Hunt, “A three-dimensional tunnel model for calculation of train-induced ground vibration”, *Journal of Sound and Vibration* **294(4-5)**, 678-705 (2006).

[6] J.A. Forrest and H.E.M. Hunt, “Ground vibration generated by trains in underground tunnels”, *Journal of Sound and Vibration* **294(4-5)**, 706-736 (2006).

[7] K.F. Riley, M.P. Hobson and S.J. Bence, *Mathematical methods for physics and engineering*. Cambridge University Press, Cambridge, 2000.

[8] R.D. Blevins, *Formulas for natural frequency and mode shape*, Robert E. Krieger Publishing, Florida, 1984.